Contribution from the Department of Chemistry,
Texas A&M University, College Station, Texas 77843

Electron-Transfer Thermodynamics and Bonding for the Superoxide ($O_2^{\bullet-}$), Dioxygen ($^{\bullet}O_2^{\bullet}$), and Hydroxyl ($^{\bullet}OH$) Adducts of (Tetrakis(2,6-dichlorophenyl)porphinato)iron, -manganese, and -cobalt in Dimethylformamide

Paul K. S. Tsang and Donald T. Sawyer*

Received April 18, 1989

The electrochemistry, spectroscopy, and magnetic moment of the superoxide ion adduct of (tetrakis(2,6-dichlorophenyl)porphinato)iron, $(Cl_8TPP)Fe(O_2)^-$, and its Mn and Co analogues, $(Cl_8TPP)Mn(O_2)^-$ and $(Cl_8TPP)Co(O_2)^-$, establish that their electron-transfer oxidations and reductions are dioxygen-centered rather than metal-centered. These $O_2^{\bullet-}$ adducts have a covalent bond that results from coupling between an unpaired d electron of the metal and an unpaired p electron of $O_2^{\bullet-}$. The valence-electron hybridization for the iron atom in $(Cl_8TPP)Fe(O_2)^-$ is d^5sp^2 (three covalent iron bonds and $S = {}^5/_2$), and the PFe–OO^- (P = porphinato) covalent bond energy (ΔH_{DBE}) is 20 kcal mol^{-1}. Similar conclusions are made for the $^{\bullet}O_2^{\bullet}$ and $^{\bullet}OH$ adducts for these metalloporphyrins.

The enzymatic activation of O_2 in aerobic organisms is the focus of much research in chemistry and biology. The cytochromes P-450 are especially important for an understanding of the O–O bond cleavage and activation mechanism. An overall reaction cycle for this heme-containing enzyme is presented in Scheme I.[1-3] After the first one-electron reduction and dioxygen-adduct formation the subsequent steps are not well understood. In an effort to obtain a better understanding of the second one-electron reduction and substrate-oxygenation steps, iron–porphyrin models have been used as simple chemical analogues for the heme active site.

The neutral, diamagnetic $PFe(O_2)$ species normally is represented as a covalent dioxygen adduct $[PFe^{II}(O_2)]$ or as an ion-pair $PFe^{III}(O_2^{\bullet-})$; the latter has been favored in much of the literature on oxyhemoglobin. One-electron reduction of $PFe(O_2)$ gives $PFe(O_2)^-$, which also can be generated by two chemical paths.[4-6]

$$PFe + O_2 + e^- \rightarrow PFe(O_2)^- \quad (1a)$$

$$[PFe]^- + O_2 \rightarrow PFe(O_2)^- \quad (1b)$$

$$PFeCl + 2O_2^{\bullet-} \rightarrow PFe(O_2)^- + O_2 + Cl^- \quad (1c)$$

The $PFe(O_2)^-$ complex has been formulated as $PFe^{III}(O_2^{2-})$ on the basis of vibrational, magnetic, spectroscopic, and electrochemical characterizations,[4-11] but an adduct form, $PFe^{II}(O_2^{\bullet-})^-$, has not been excluded.[12]

The basis for an ionic $PFe^{III}(O_2^{2-})^-$ formulation is that the vibrational frequency of the bound dioxygen is 806 cm^{-1} for $(OEP)Fe(O_2)^-$ (OEP = octaethylporphyrin dianion),[4] which corresponds better to a peroxide classification (Na_2O_2, 766 cm^{-1})[13] than to a superoxide formulation (KO_2, 1145 cm^{-1};[14] $O_2^{\bullet-}$(g), 1065 cm^{-1}).[15] However, the vibrational frequencies of HOOH (877 cm^{-1})[16] and HOO^- (836 cm^{-1})[17] also are in the range of those for $(OEP)Fe(O_2)^-$, but the bonding in HOOH and HOO^- is covalent (H–OO–H and H–OO^-) and not ionic (H^+–O–O^+H and H^+O–O^-). The $(PFe^{III})^+$ and O_2^{2-} oxidation levels also are incompatible, given that the formal reduction potential of the $(PFe^{III})^+/PFe^{II}$ couple ($E^{\circ\prime}$ = –0.15 V vs SCE) is more positive than that for the $O_2/O_2^{\bullet-}$ couple ($E^{\circ\prime}$ = –0.85 V vs SCE) and the $O_2^{\bullet-}/O_2^{2-}$ couple ($E^{\circ\prime} < -3.0$ V vs SCE); outer-sphere electron transfer from $O_2^{\bullet-}$ or O_2^{2-} to $(PFe^{III})^+$ is favored.

Scheme I. Cytochrome P-450 Reaction Cycle (P = Protoporphyrin IX Dianion, RH = Substrate, R'S^- = Cysteinato-*S*; LS = Low Spin, HS = High Spin)

$$[(R'S)PFe]_{LS} + RH \longrightarrow [(R'S)PFe(RH)]_{HS}$$

$$[(R'S)PFe(RH)]_{HS} + e^- \longrightarrow [(R'S)PFe(RH)]^-$$

$$[(R'S)PFe(RH)]^- + O_2 \longrightarrow [(R'S)PFe(RH)(O_2)]^-$$

$$[(R'S)PFe(RH)(O_2)]^- + e^- \xrightarrow{2H^+} [(R'S)(P)Fe{=}O(RH)(OH_2)]$$

Compound I

$$\downarrow$$

$$[(R'S)PFe]_{LS} + ROH + H_2O$$

Moreover, nuclear magnetic resonance and electrochemical experiments have shown that the combination of $(PFe^{III})^+$ and ^-OH (a less powerful reductant than O_2^{2-}) results in electron transfer to give the ferrous porphyrin $[PFe^{II}]$.[18-20] The oxidation of ^-OH in the presence of transition-metal complexes has indicated that electron transfer is oxygen-centered with the oxidized ligand stabilized through a coupling of the unpaired p electron of oxygen and an unpaired d electron of the transition metal to give a d–p covalent bond.[19] Ligand-centered electron transfer stabilized through covalent-bond formation also has been demonstrated in metal–dithiolate complexes, where a sulfur–metal bond is formed when the complex is oxidized.[21] Oxidation of metal–catechol[22-24]

(1) Dawson, J. H.; Eble, K. S. *Adv. Inorg. Bioinorg. Mech.* **1986**, *4*, 1.
(2) *Cytochrome P-450: Structure, Mechanism, and Biochemistry*; Ortiz de Montellano, P. R., Ed.; Plenum: New York, 1986.
(3) Gunegerich, F. P.; MacDonald, T. C. *Acc. Chem. Res.* **1984**, *17*, 9.
(4) McCandlish, E.; Miksztal, A. R.; Nappa, M.; Sprenger, A. Q.; Valentine, J. S.; Strong, J. D.; Spiro, T. G. *J. Am. Chem. Soc.* **1980**, *102*, 4268.
(5) Welborn, C. H.; Dolphin, D.; James, B. R. *J. Am. Chem. Soc.* **1981**, *103*, 2869.
(6) Reed, C. A. In *Electrochemical and Spectrochemical Studies of Biological Redox Compounds*; Kadish, K. M., Ed.; Advances in Chemistry 201; American Chemical Society: Washington, DC 1982; pp 333–356.
(7) Valentine, J. S.; McCandlish, E. In *Frontiers of Biological Energetics: Electrons to Tissues*; Dutton, P. L., Leigh, J. S., Scarpa, A., Eds.; Academic: New York, 1978; Vol. 2, pp 933–939.
(8) Shirazi, A.; Goff, H. M. *J. Am. Chem. Soc.* **1982**, *104*, 6318.
(9) Jones, S. E.; Srivatsa, G. S.; Sawyer, D. T.; Traylor, T. G.; Mincey, T. C. *Inorg. Chem.* **1983**, *22*, 3903.
(10) Friant, P.; Goulon, J.; Fischer, J.; Ricard, L.; Schappacher, M.; Weiss, R.; Momenteau, M. *Nouv. J. Chim.* **1985**, *9*, 33.
(11) Burstyn, J. N.; Roe, J. A.; Miksztal, A. R.; Shaevity, B. A.; Lang, G.; Valentine, J. S. *J. Am. Chem. Soc.* **1988**, *110*, 1382.
(12) Koltover, V. K.; Koifman, O. I.; Khenkin, A. M.; Shteinman, A. A. *Izv. Akad. Nauk SSSR, Ser. Khim.* **1978**, *7*, 1690.
(13) Evans, J. C. *J. Chem. Soc., Dalton Trans.* **1969**, 682.
(14) Crighton, J. A.; Lippincote, E. R. *J. Chem. Phys.* **1964**, *40*, 1779.
(15) Boness, M. J. W.; Schultz, G. J. *Phys. Rev. A* **1970**, *2*, 2182.
(16) Shimanouchi, T. *J. Phys. Chem. Ref. Data* **1974**, *6*, 993.
(17) (a) Simon, A.; Kriegsman, H. *Naturwissenschaften* **1955**, *42*, 14. (b) Knop, O.; Figuere, P. A. *Can. J. Chem.* **1959**, *37*, 1794.
(18) Shin, K.; Kramer, S. K.; Goff, H. M. *Inorg. Chem.* **1987**, *26*, 4103.
(19) Tsang, P. K. S.; Cofrê, P.; Sawyer, D. T. *Inorg. Chem.* **1987**, *26*, 3604.
(20) Srivatsa, G. S.; Sawyer, D. T. *Inorg. Chem.* **1985**, *24*, 1732.
(21) Sawyer, D. T.; Srivatsa, G. S.; Bodini, M. E.; Schaefer, W. P.; Wing, R. M. *J. Am. Chem. Soc.* **1986**, *108*, 936.
(22) Jones, S. E.; Leon, L. E.; Sawyer, D. T. *Inorg. Chem.* **1982**, *21*, 3692.
(23) Bodini, M. E.; Copia, G.; Robinson, R.; Sawyer, D. T. *Inorg. Chem.* **1983**, *22*, 126.

0020-1669/90/1329-2848$02.50/0

and manganese[25] compounds also involves ligand-centered electron transfer with covalent-bond formation between the metal center and the oxidized oxygen-donor ligands.

These considerations have prompted an assessment of the electron-transfer thermodynamics associated with the one-electron reduction product of $PFe(O_2)$ and thereby gain insight into the site of electron transfer and to the nature of the metal–oxygen bonding. Electrochemistry, optical spectroscopy, and magnetic susceptibility measurements have been employed to characterize metal–oxygen interactions for the $O_2^{\bullet-}$, $^{\bullet}O_2^{\bullet}$, and $^{\bullet}OH$ adducts of $(Cl_8TPP)Fe$, $(Cl_8TPP)Mn$, and $(Cl_8TPP)Co$.

Experimental Section

Equipment. Cyclic voltammetry was accomplished with a Bioanalytical Systems Model CV-27 instrument and a Houston Instruments Model 200 XY recorder. The electrochemical measurements were made with a microcell assembly (10-mL capacity) that was adapted to use a glassy-carbon working electrode (area 0.09 cm^2), a platinum-wire auxiliary electrode (contained in a glass tube with a medium-porosity glass frit and filled with a concentrated solution of supporting electrolyte), and a Ag/AgCl reference electrode (filled with aqueous tetramethylammonium chloride solution and adjusted to 0.00 V vs SCE)[26] with a solution junction via a Pyrex glass tube closed with a cracked-glass bead (soft glass) that was contained in a luggin capillary. Controlled-potential electrolysis was accomplished with a Princeton Applied Research Model 173/179 potentiostat/digital coulometer. A glassy-carbon plate and a platinum-mesh auxiliary electrode (embedded in anhydrous Na_2CO_3 to remove protons produced from the anode reaction) were used for the controlled-potential electrolysis experiments. The stoichiometric electrochemical generation of $O_2^{\bullet-}$ in the presence of the metalloporphyrins required less than 1 min with an O_2 (1 atm)-saturated solution.

The UV–visible spectrophotometric measurements were made with a Hewlett-Packard Model 8450A diode-array spectrophotometer. Magnetic susceptibilities were determined by the Evans method[27-29] with a Varian XL-200 NMR spectrometer. Air-sensitive compounds were synthesized and handled in a Vacuum Atmospheres Model HE-493 Dri-Lab with a Model HE-493 Dri-Train system under an argon atmosphere. All experiments were performed at 23 ± 1 °C.

Chemicals and Reagents. Dimethylformamide (DMF) and acetonitrile (MeCN), "distilled-in-glass" grade from Burdick and Jackson, were used without further purification. Tetraethylammonium perchlorate (TEAP) was vacuum-dried for 24 h prior to use. Tetrabutylammonium hydroxide $[(Bu_4N)OH]$ was obtained from Aldrich as a 25% solution in methanol, and its concentration was determined by acid–base titration. All other solvents and chemicals were the highest purity commercially available and were used as received.

Synthesis of Complexes. Tetramethylammonium superoxide $[(Me_4N)O_2]$ was prepared by combination of KO_2 and $(Me_4N)OH{\cdot}H_2O$ and subsequent extraction in liquid ammonia.[30,31] 5,10,15,20-Tetrakis(2,6-dichlorophenyl)porphine (Cl_8TPPH_2) was synthesized from 2,4,6-collidine[32,33] and was used to prepare $(Cl_8TPP)MnCl$,[34] $(Cl_8TPP)FeCl$,[33,34] $(Cl_8TPP)Co$,[34] and $(Cl_8TPP)Zn$.[32,35] The perchlorate salts $(Cl_8TPP)Mn(ClO_4)$ and $(Cl_8TPP)Fe(ClO_4)$ were prepared by metathesis of the respective chloride salts with 1 equiv of anhydrous $AgClO_4$ in hot toluene.[36]

Results

Electrochemistry. The electrochemical oxidation of ^-OH at a glassy-carbon electrode in DMF occurs at +0.65 V vs SCE.[37,38] In the presence of $(Cl_8TPP)Zn$, a transition-metal complex with a filled d^{10} subshell, the oxidation of ^-OH occurs at essentially the same potential ($E^{\circ\prime}$ = +0.66 V). The formal reduction potential for the $O_2/O_2^{\bullet-}$ couple in DMF is −0.88 V vs SCE; in the presence of $(Cl_8TPP)Zn$ with 1 equiv of ^-OH, oxidation of $O_2^{\bullet-}$ occurs at −0.86 V.

The cyclic voltammograms of $(Cl_8TPP)Fe$ and its 1:1 combination with ^-OH are shown in Figure 1a,b, respectively. The combination of 10 equiv of ^-OH with $(Cl_8TPP)Fe$ exhibits a cyclic voltammogram that is a composite of that for $[(Cl_8TPP)Fe + {}^-OH]$ and that due to excess ^-OH (irreversible oxidations at 0.00 and +0.65 V). Bubbling O_2 (1 atm) through a solution of $[(Cl_8TPP)Fe + 10(^-OH)]$, followed by deaeration with Ar, gives a product solution that exhibits the cyclic voltammogram shown in Figure 1c $[(Cl_8TPP)Fe^{II}$ and other sterically hindered ferrous porphyrins preclude μ-O_2 dimer formation]. Reversal of a positive scan after the oxidation peak at −0.31 V yields a new reduction

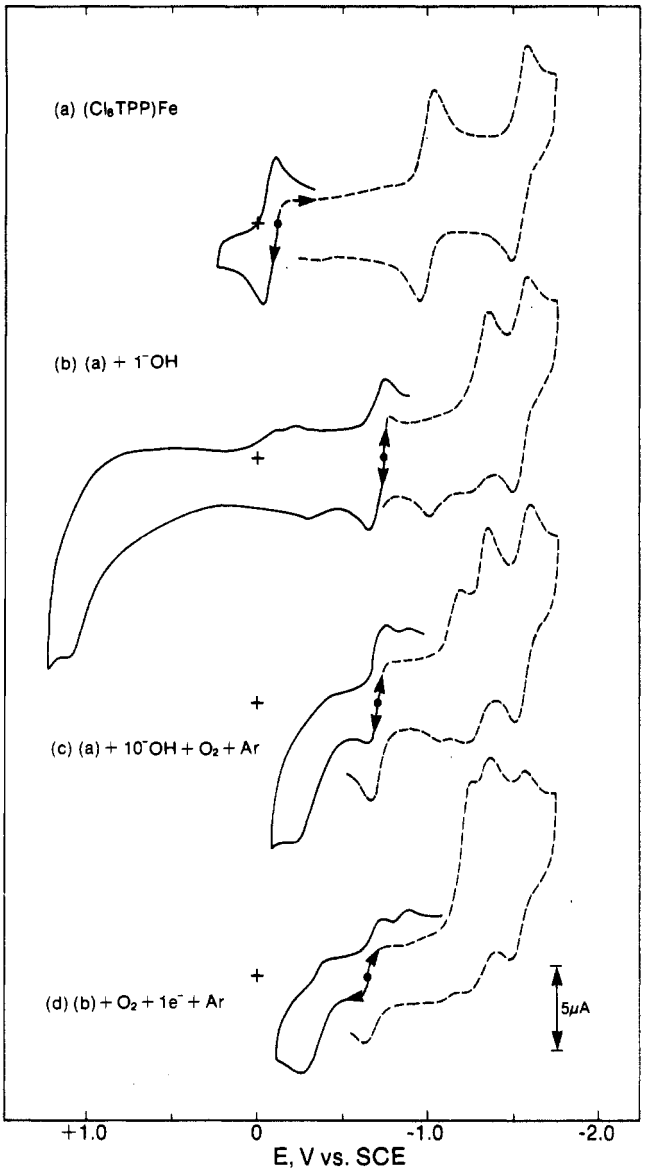

Figure 1. Cyclic voltammograms in DMF (0.1 M TEAP) of (a) 0.5 mM $(Cl_8TPP)Fe$, (b) 0.5 mM $(Cl_8TPP)Fe$ plus 0.5 mM $(Bu_4N)OH$, (c) the product from the combination of 0.5 mM $(Cl_8TPP)Fe$, 5.0 mM $(Bu_4N)OH$, and O_2 (1 atm, ca. 2 min.), followed by deaeration with Ar, and (d) deaerated one-electron reduction product of 0.5 mM $(Cl_8TPP)Fe$, 1 equiv of $(Bu_4N)OH$, and O_2 (1 atm) [scan rate 0.1 V s^{-1}; glassy-carbon electrode (GCE)].

(24) Haga, M.-A.; Rodsworth, E. A.; Lever, A. B. P. *Inorg. Chem.* **1986**, *25*, 447.
(25) Richert, S. A.; Tsang, P. K. S.; Sawyer, D. T. *Inorg. Chem.* **1988**, *27*, 1814.
(26) Sawyer, D. T.; Roberts, J. L., Jr. *Experimental Electrochemistry for Chemists*; Wiley: New York, 1974; pp 44–46, 144–145, 336–339.
(27) Evans, D. F. *J. Chem. Soc.* **1959**, 2003.
(28) Carlin, R. L. *Magnetochemistry*; Springer-Verlag: New York, 1986.
(29) Brevard, C.; Granger, P. *Handbook of High Resolution Multinuclear NMR*; Wiley-Interscience: New York, 1981.
(30) Sawyer, D. T.; Calderwood, T. S.; Yamaguchi, K.; Angelis, C. T. *Inorg. Chem.* **1982**, *22*, 2577.
(31) Yamaguchi, K.; Calderwood, T. S.; Sawyer, D. T. *Inorg. Chem.* **1986**, *25*, 1289.
(32) Badger, G. M.; Jones, R. A.; Laslett, R. L. *Aust. J. Chem.* **1964**, *17*, 1028.
(33) Kobayashi, H.; Higuchi, T.; Kaizu, Y.; Osada, H.; Aoki, M. *Bull. Chem. Soc. Jpn.* **1975**, *48*, 3137.
(34) Alder, A. D.; Longo, F. R.; Varadi, V. *Inorg. Synth.* **1976**, *16*, 213.
(35) Traylor, P. S.; Dolphin, D.; Traylor, T. G. *J. Chem. Soc., Chem. Commun.* **1984**, 279.
(36) Hill, C. L.; Williamson, M. M. *Inorg. Chem.* **1985**, *24*, 2836.
(37) The SCE is +0.24 V vs NHE.
(38) All potentials are versus SCE unless otherwise stated.

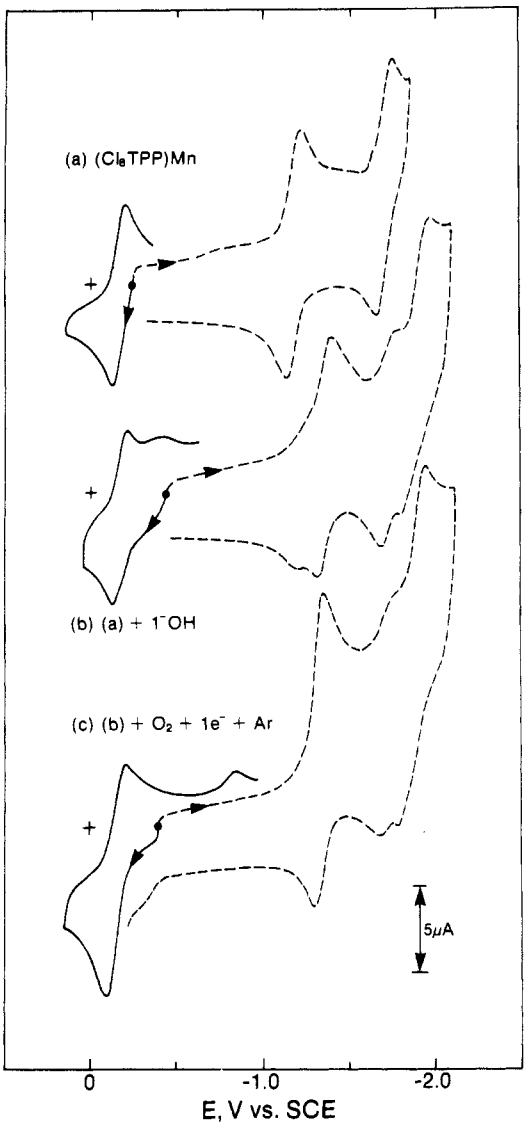

Figure 2. Cyclic voltammograms in DMF (0.1 M TEAP) of (a) 0.5 mM $(Cl_8TPP)Mn$, (b) 0.5 mM $(Cl_8TPP)Mn$ plus 0.5 mM $(Bu_4N)OH$, and (c) deaerated one-electron reduction product of 0.5 mM $(Cl_8TPP)Mn$, 0.5 mM $(Bu_4N)OH$, and O_2 (1 atm) [scan rate 0.1 V s^{-1}; GCE].

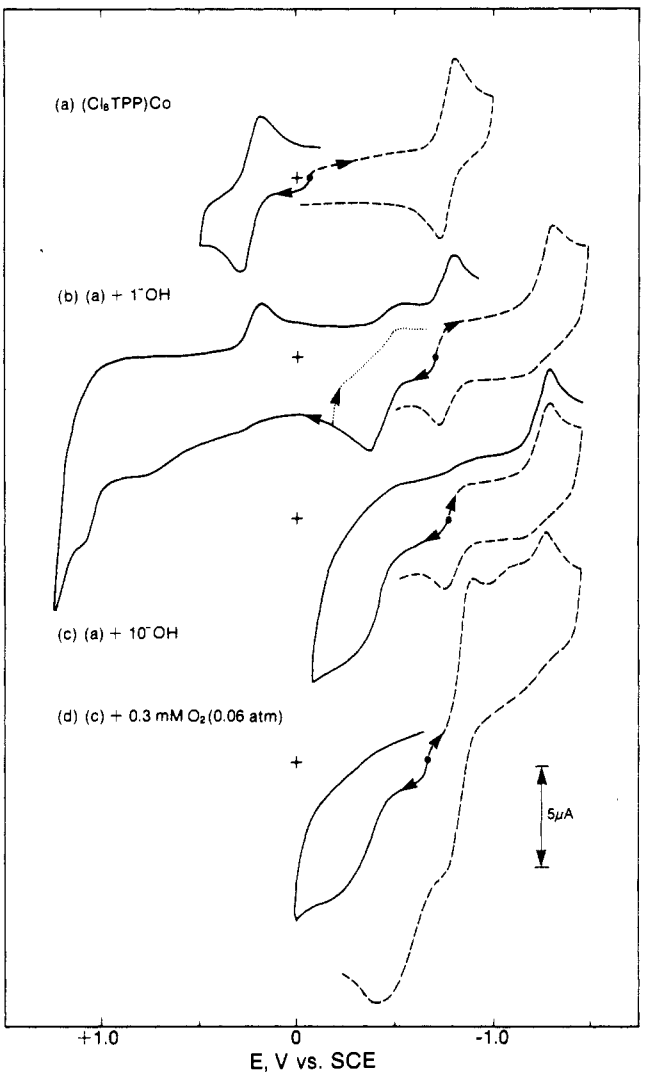

Figure 3. Cyclic voltammograms in DMF (0.1 M TEAP) of (a) 0.5 mM $(Cl_8TPP)Co$, (b) 0.5 mM $(Cl_8TPP)Co$ plus 0.5 mM $(Bu_4N)OH$, (c) 0.5 mM $(Cl_8TPP)Co$ plus 5 mM $(Bu_4N)OH$, and (d) 0.5 mM $(Cl_8TPP)Co$ plus 5 mM $(Bu_4N)OH$ and 0.3 mM O_2 (0.06 atm) [scan rate 0.1 V s^{-1}; GCE].

peak at −0.88 V that is not observed for an initial negative scan. When 1–3 equiv of ^-OH is combined with $(Cl_8TPP)Fe$, the addition of O_2 results in the formation of a product that has electrochemistry identical with that for the 1:1 combination of $(Cl_8TPP)Fe(ClO_4)$ and ^-OH.

Figure 1d illustrates the cyclic voltammogram for the solution that results from the combination of $(Cl_8TPP)Fe$, 1 equiv of ^-OH, O_2 (1 atm), and 1 equiv of electrons (controlled-potential coulometry at −0.96 V) and subsequent deaeration with Ar. Reversal of a positive scan after the −0.36-V oxidation peak results in a reduction at −0.90 V that is not observed for an initial negative scan. A product solution with identical electrochemical properties is obtained when 2 equiv of tetramethylammonium superoxide $[(Me_4N)O_2]$ is combined [either with or without ^-OH present because dissolution of $(Me_4N)O_2$ yields $O_2^{\bullet-}$ and ^-OH][31] with $(Cl_8TPP)Fe(ClO_4)$ in DMF or MeCN.

Figure 2 illustrates the electrochemistry for $(Cl_8TPP)Mn$ and its 1:1 combination with ^-OH; with additional ^-OH equivalents the small oxidation wave at −0.43 V becomes a full two-electron process and a multiple-electron oxidation at +0.19 V emerges. The combination of $(Cl_8TPP)Mn$, 1 equiv of ^-OH, O_2 (1 atm), and 1 equiv of electrons (controlled-potential coulometry at −0.96 V) yields a product with the cyclic voltammogram of Figure 2c. When an initial positive scan is reversed after the −0.13-V oxidation peak, a reduction peak occurs at −0.85 V that is not observed for an initial negative scan. When the negative scan is reversed after the two-electron reduction at −1.35 V, the reoxidation at −0.62 V is a one-electron reversible process. Identical results are obtained if 1 equiv of ^-OH is not used in the electrosynthesis solution.

The cyclic voltammograms of $(Cl_8TPP)Co$ and its 1:1 and 1:10 combinations with ^-OH are shown in Figure 3. For the last system (curve c) the anodic current at potentials more positive than 0.00 V is due to the excess ^-OH. Curve d of Figure 3 illustrates the cyclic voltammogram for a combination of 0.5 mM $(Cl_8TPP)Co$, 5 mM ^-OH, and 0.3 mM O_2. When an initial negative scan is reversed at −1.00 V, the oxidation peak at −0.40 V is not observed. Reductive electrolysis of a solution that contains $(Cl_8TPP)Co$ or $[(Cl_8TPP)Co + {}^-OH]$ and O_2 gives a precipitate, as does reduction of $(Cl_8TPP)Co$.

The electrochemistry of O_2 and of O_2 in combination with $(Cl_8TPP)Zn$, $(Cl_8TPP)Fe$, $(Cl_8TPP)Mn$, and $(Cl_8TPP)Co$ is illustrated in Figure 4. The initial oxidation at 0.00 V for $[(Cl_8TPP)Fe + O_2$ (1 atm)] is slightly more positive than that for $(Cl_8TPP)Fe$ in the absence of O_2 ($E_{p,a}$ = −0.02 V). Within 20 min after preparation this system hydrolyzes to give about 10% $(Cl_8TPP)FeOH$. In contrast, a solution of $(Cl_8TPP)Fe$ and 1,2-dimethylimidazole in the presence of O_2 (1 atm) is stable for at least 5 h.

Electronic Spectroscopy. Addition of 1 equiv of ^-OH to $(Cl_8TPP)Zn$ causes its Soret band to shift from 426 to 440 nm

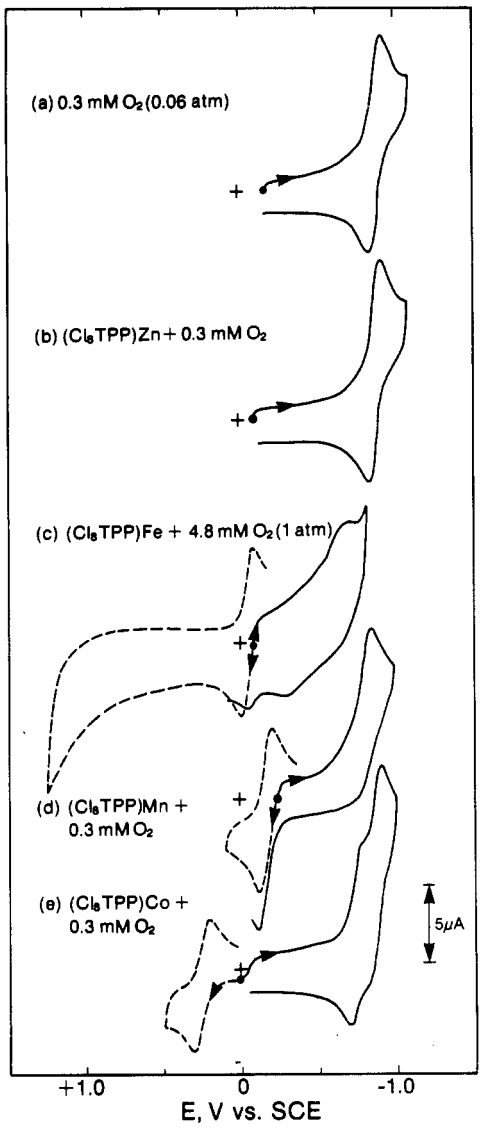

Figure 4. Cyclic voltammograms in DMF (0.1 M TEAP) of (a) 0.3 mM O_2 (0.06 atm), (b) 0.5 mM $(Cl_8TPP)Zn$ plus 0.3 mM O_2, (c) 0.5 mM $(Cl_8TPP)Fe$ plus 4.8 mM O_2 (1 atm), (d) 0.5 mM $(Cl_8TPP)Mn$ plus 0.3 mM O_2, and (e) 0.5 mM $(Cl_8TPP)Co$ plus 0.3 mM O_2 [scan rate 0.1 V s^{-1}; GCE].

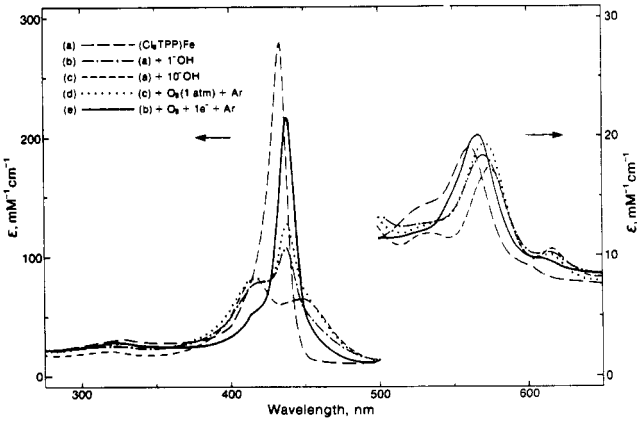

Figure 5. Absorption spectra in DMF (0.1 M TEAP) of (a) $(Cl_8TPP)Fe$, (b) $(Cl_8TPP)Fe$ plus 1 equiv of $(Bu_4N)OH$, (c) $(Cl_8TPP)Fe$ plus 10 equiv of $(Bu_4N)OH$, (d) deaerated product from the combination of $(Cl_8TPP)Fe$, 10 equiv of $(Bu_4N)OH$, and O_2 (1 atm, ca. 2 min), and (e) deaerated one-electron reduction product from the combination of $(Cl_8TPP)Fe$, 1 equiv of $(Bu_4N)OH$, and O_2 (1 atm).

and its visible band to shift from 560 to 574 nm. The deaerated one-electron reduction product of $(Cl_8TPP)Zn$ in combination with

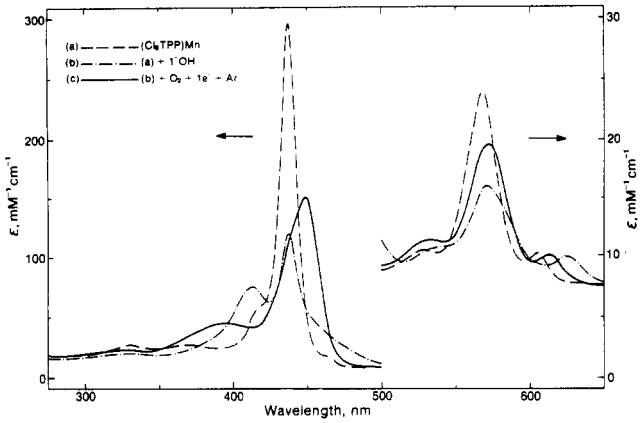

Figure 6. Absorption spectra in DMF (0.1 M TEAP) of (a) $Cl_8TPP)Mn$, (b) $(Cl_8TPP)Mn$ plus 1 equiv of $(Bu_4N)OH$, and (c) deaerated one-electron reduction product from the combination of $(Cl_8TPP)Mn$, 1 equiv of $(Bu_4N)OH$, and O_2 (1 atm).

Table I. Magnetic Moments for $(Cl_8TPP)Fe(ClO_4)$ and $(Cl_8TPP)Mn(ClO_4)$ and for Their Various Reaction Products in DMF (23 °C)

compd[a]	μ_B, $\pm 0.30\ \mu_B$
A. Fe	
$(Cl_8TPP)Fe^{III}(ClO_4)$	5.15
$(Cl_8TPP)Fe^{III}(ClO_4)$	4.43[b]
$(Cl_8TPP)Fe^{III}(ClO_4) + {}^-OH \rightarrow (Cl_8TPP)Fe^{III}–OH$	5.24 (5.15)[b]
$(Cl_8TPP)Fe^{III}(ClO_4) + 3({}^-OH) \rightarrow [(HO^-)(Cl_8TPP)Fe^{III}–OH]^-$	3.83[b]
$(Cl_8TPP)Fe^{II}$	4.90
$(Cl_8TPP)Fe^{II} + {}^-OH$	5.03
$(Cl_8TPP)Fe^{II} + 10({}^-OH) \rightarrow (Cl_8TPP)Fe^{II}({}^-OH)^-$	3.83
$(Cl_8TPP)Fe^{II} + 10({}^-OH) + O_2 + Ar \rightarrow (Cl_8TPP)Fe^{IV}(OH)(OO^-)$	2.91
$(Cl_8TPP)Fe^{II} + {}^-OH + O_2 + e^- + Ar \rightarrow (Cl_8TPP)Fe^{III}–OO^-$	5.57
B. Mn	
$(Cl_8TPP)Mn^{III}(ClO_4)$	4.57
$(Cl_8TPP)Mn^{III}(ClO_4) + {}^-OH \rightarrow (Cl_8TPP)Mn^{III}–OH$	4.57
$(Cl_8TPP)Mn^{II}$	5.77
$(Cl_8TPP)Mn^{II} + {}^-OH$	5.28
$(Cl_8TPP)Mn^{II} + 10({}^-OH) \rightarrow (Cl_8TPP)Mn^{II}({}^-OH)^-$	5.66
$(Cl_8TPP)Mn^{II} + 10({}^-OH) + O_2 + Ar \rightarrow (Cl_8TPP)Mn^{II}({}^-OH)^-$	5.76
$(Cl_8TPP)Mn^{II} + {}^-OH + O_2 + e^- + Ar \rightarrow (Cl_8TPP)Mn^{III}–OO^-$	4.98

[a] The superscript Roman numerals indicate the covalence (number of covalent bonds) for the metal, *not* the oxidation state. [b] In MeCN.

1 equiv of ^-OH and O_2 (1 atm) has an optical spectrum that is almost identical with that of $(Cl_8TPP)Zn$ with 1 equiv of ^-OH. The UV–visible spectra for $(Cl_8TPP)Fe$ and its combinations with various oxygen species are shown in Figure 5. The spectrum of $(Cl_8TPP)Fe$ in the presence of 10 equiv of ^-OH and O_2 (1 atm) has a greater intensity than that of a deaerated solution (Figure 5d); combination of the latter with O_2 (1 atm) yields a product solution with the same spectrum as the $[(Cl_8TPP)Fe + 10(^-OH) + O_2$ (1 atm)] solution.

The UV–visible absorption spectra of $(Cl_8TPP)Mn$, its 1:1 combination with ^-OH, and the one-electron reduction product of the combination $[(Cl_8TPP)Mn + O_2$ (1 atm)] are presented in Figure 6. In DMF the UV–visible absorption spectra of $(Cl_8TPP)Zn$, $(Cl_8TPP)Co$, and $(Cl_8TPP)Mn$ are unaffected by the presence of O_2 (1 atm). However, exposure of $(Cl_8TPP)Fe$ to O_2 (1 atm) results in a split Soret band (422, 434 nm) and a single visible band at 564 nm; within 15 min a Soret band at 410 nm begins to appear, which is characteristic of $(Cl_8TPP)Fe(OH)$.

Magnetic Susceptibilties. The apparent solution magnetic moments for $(Cl_8TPP)Fe(ClO_4)$, $(Cl_8TPP)Mn(ClO_4)$, and for their various reaction products in DMF are summarized in Table

Table II. Redox Thermodynamics for Oxygen Species and Their Adducts with $(Cl_8TPP)Fe$, $(Cl_8TPP)Mn$, and $(Cl_8TPP)Co$ in DMF[a]

	$E^{\circ\prime}$, V vs SCE[b]	$-\Delta G_{BF}$, kcal/mol[c]
$2(^-OH) \rightarrow O^{\bullet-} + H_2O + e^-$	+0.65	
$O^{\bullet-} \rightarrow {}^\bullet O^\bullet + e^-$	+0.43	
$O_2 + e^- \rightarrow O_2^{\bullet-}$	−0.88	
$O_2^- + H_2O + e^- \rightarrow H\text{-}OO^- + {}^-OH$	−1.64	
$PZn^{II} + 2(^-OH) \rightarrow PZn^{II} + O^{\bullet-} + H_2O + e^-$	+0.66	
$PZn^{II} + O_2^{\bullet-} \rightarrow PZn^{II} + O_2 + e^-$	−0.86	
$PFe^{II} + {}^-OH \rightarrow PFe^{III}\text{–}OH + e^-$ (d^6sp, $S=4/2$ → d^5sp^2, $S=5/2$)	−0.70	31
$PFe^{III}\text{–}OH + {}^-OH \rightarrow [(HO^-)PFe^{III}\text{–}OH]^-$ (d^5sp^2, $S=3/2$)		
$PMn^{II} + {}^-OH \rightarrow PMn^{III}\text{–}OH + e^-$ (d^5sp, $S=5/2$ → d^5sp, $S=4/2$)	−0.43	25
$(PCo^{II\bullet}) + {}^-OH \rightarrow PCo^{III}\text{–}OH + e^-$ (d^7sp, $S=1/2$ → d^7sp, $S=0$)	−0.43	25
$PFe^{III}\text{–}OH + {}^-OH \rightarrow PFe^{IV}{=}O + H_2O + e^-$ (d^6sp, $S=2/2$)	0.00	
$PMn^{III}\text{–}OH + {}^-OH \rightarrow PMn^{IV}{=}O + H_2O + e^-$ (d^5sp, $S=3/2$)	<−0.43	
$PMn^{IV}{=}O + 4(^-OH) \rightarrow PMn^{IV}{=}O + O_2 + 2H_2O + 4e^-$	+0.09	
$PCo^{III}\text{–}OH + {}^-OH \rightarrow PCo^{III}\text{–}O^\bullet + H_2O + e^-$ (d^7sp, $S=1/2$)	+0.43	
$PFe^{III}\text{–}OO^- \rightarrow PFe^{II} + O_2 + e^-$ (d^5sp^2, $S=5/2$)	−0.36	12
$PFe^{IV}(OH)(OO^-) \rightarrow PFe^{III}\text{–}OH + O_2 + e^-$ (d^6sp, $S=2/2$)	−0.33	12
$PMn^{III}\text{–}OO^- \rightarrow PMn^{II} + O_2 + e^-$ (d^5sp, $S=4/2$)	−0.13	17
$PCo^{III}\text{–}OO^- \rightarrow (PCo^{II})^\bullet + O_2 + e^-$ (d^7sp, $S=0$)	−0.55	7
$PFe^{IV}(O_2) + e^- \rightarrow PFe^{III}\text{–}OO^-$ (d^6sp, $S=0$)	−0.57	

[a] Proposed valence-electron hybridizations for the metal centers are below the metal complex; the superscript Roman numerals indicate the covalence (number of covalent bonds) for the metal, *not* the oxidation state. [b] $E_{SCE} = E_{NHE} - 0.24$ V. [c] $-\Delta G_{BF} = [E^{\circ\prime}(Zn, X^\bullet/Zn, X^-) - E^{\circ\prime}(M\text{–}X/M, X^-)] \times 23.1$ kcal.

I. The addition of ^-OH to $(Cl_8TPP)Fe(ClO_4)$ in DMF does not alter its magnetic moment.

Discussion and Conclusions

On the basis of the electrochemical, spectroscopic, and magnetic susceptibility results, the redox thermodynamics for various oxygen species and their adducts with $(Cl_8TPP)Zn$, $(Cl_8TPP)Fe$, $(Cl_8TPP)Mn$, and $(Cl_8TPP)Co$ are proposed and summarized in Table II. [The Roman numerial superscript associated with the transition metal in the present discussion of electron-transfer thermodynamics indicates the covalence (number of covalent bonds) for the metal, *not* the oxidation state or number.][39]

^-OH Adducts. The oxidation of ^-OH in the presence of $(Cl_8TPP)Zn^{II}$ occurs at a slightly more positive potential than that for free ^-OH. This is consistent with the metal center delocalizing the electron density of ^-OH to make removal of an electron more difficult. When ^-OH adducts of metalloporphyrins that contain partially filled d subshells are oxidized, the potentials are less positive than that for free ^-OH oxidation. This facilitated oxidation of ^-OH is due to the stabilization of the oxidized product ($^\bullet OH$) via formation of a d–p covalent bond between the unpaired p electron of $^\bullet OH$ and an unpaired d electron of the metal center. This interpretation is consistent with previous reports that have demonstrated d–p covalent bond formation in the oxidation of ^-OH adducts of transition-metal[19] and metal–dithiolate complexes.[21]

Further support for this conclusion is provided by the magnetic data for the combination of $(Cl_8TPP)Fe^{III}(ClO_4)$ and ^-OH (Table I). The intermediate spin value for $(Cl_8TPP)Fe^{III}(ClO_4)$ in MeCN is consistent with values for perchlorate salts of ferric porphyrins in noncoordinating solvents.[40] With the addition of 1 equiv of ^-OH the $(Cl_8TPP)Fe^{III}(ClO_4)$ complex is reduced to $(Cl_8TPP)Fe^{II}$, which couples with the resulting $^\bullet OH$ to form $(Cl_8TPP)Fe^{III}\text{–}OH$. Reduction of PFe^+ by ^-OH has been demonstrated previously,[18,20] but the formation of a PFe–OH covalent bond and its electronic character have not been discussed.

Additional perspective is provided by recasting the standard-state reduction-potential half-reactions for Fe(III/II), Mn(III/II), and Co(III/II) to accommodate their interaction with an aqueous matrix at pH 0.

$$[(H_2O)_5Fe^{III}\text{–}OH]^{2+} + H_3O^+ + e^- \rightarrow [(H_2O)_4Fe^{II}]^{2+} + 3H_2O \quad (d^5sp^2,\ S=5/2 \rightarrow d^6sp,\ S=4/2)$$
$$-\Delta G_{BF} = 45 \text{ kcal}, \quad E^\circ = +0.77 \text{ V vs NHE} \qquad (2)$$

$$[(H_2O)_5Mn^{III}\text{–}OH]^{2+} + H_3O^+ + e^- \rightarrow [(H_2O)_4Mn^{II}]^{2+} + 3H_2O \quad (d^5sp,\ S=4/2 \rightarrow d^5sp,\ S=5/2)$$
$$-\Delta G_{BF} = 28 \text{ kcal}, \quad E^\circ = +1.51 \text{ V vs NHE} \qquad (3)$$

$$[(H_2O)_5Co^{III}\text{–}OH]^{2+} + H_3O^+ + e^- \rightarrow [((H_2O)_4Co^{II})^\bullet]^{2+} + 3H_2O \quad (d^7sp,\ S=0 \rightarrow d^7sp,\ S=1/2)$$
$$-\Delta G_{BF} = 18 \text{ kcal}, \quad E^\circ = +1.92 \text{ V vs NHE} \qquad (4)$$

Each oxidized species has three covalent linkages (two $[M\text{–}OH_2]^+$ bonds and one M–OH bond). Reduction causes the M–OH bond to be broken to form an H–OH bond in a product H_2O molecule. Thus, the difference in the E° values of eqs 2–4 and that for the reduction of free $^\bullet OH$

$$^\bullet OH + H_3O^+ + e^- \rightarrow 2H_2O \qquad E^\circ = +2.72 \text{ V vs NHE} \qquad (5)$$

is a measure of the $[(H_2O)_5M\text{–}OH]^{2+}$ bond energy.[19] For example

$$-\Delta G_{BF} = [E^\circ(^\bullet OH/H_2O) - E^\circ((Fe\text{–}OH)^+)] \times 23.1 = (2.72 - 0.77)23.1 = 45 \text{ kcal} \qquad (6)$$

This and the values of 28 kcal $[(H_2O)_5Mn^{III}\text{–}OH^{2+}]$ and 18 kcal $[(H_2O)_5Co^{III}\text{–}OH^{2+}]$ are consistent with the values for the $PFe^{III}\text{–}OH$, $PMn^{III}\text{–}OH$, and $PCo^{III}\text{–}OH$ bonds (Table II); the gas-phase bond energies ($-\Delta G_{BF}$) for $Fe^+\text{–}OH$ and $Fe^+{=}O$ are 65 and 61 kcal, respectively.[41]

Recent theoretical[42-46] and experimental[19,21,25,46] reports have provided compelling arguments in support of covalent metal–ligand bonds in transition-metal complexes. Thus, metalloporphyrins (PZn, PMn, PFe, PCo) are more reasonably formulated with uncharged metal centers [$Zn(d^{10}sp)$, $Mn(d^5sp)$, $Fe(d^6sp)$, $Co(d^7sp)$] bonded via two metal–nitrogen covalent bonds with un-

(39) Sawyer, D. T. *Comments Inorg. Chem.* **1990**, *10*, 129.
(40) Scheidt, W. R.; Gouterman, M. In *Iron Porphyrins*; Lever, A. B. P., Gray, H. B., Eds.; Addison-Wesley: Reading, MA, 1983; Part I, p 119.
(41) Kang, H.; Beauchamp, J. L. *J. Am. Chem. Soc.* **1986**, *108*, 5663.
(42) Harrison, J. F. *J. Phys. Chem.* **1986**, *90*, 3313.
(43) Sanderson, R. T. *Inorg. Chem.* **1986**, *25*, 3518.
(44) Di Bella, S.; Fragala, I.; Granozzi, G. *Inorg. Chem.* **1986**, *25*, 3997.
(45) Low, J. J.; Goddard, W. A., III. *J. Am. Chem. Soc.* **1986**, *108*, 6115.
(46) Sawyer, D. T. *Comments Inorg. Chem.* **1987**, *6*, 103.

charged porphyrin [analogous to porphine (PH_2)].[39,47] There is general acceptance that porphine has two hydrogen atoms bound via covalent bonds to two pyrrole nitrogens. The magnetic moment for $(Cl_8TPP)Fe(OH)$ (5.24 μ_B) as well as other spectroscopic evidence[18] are consistent with d^5sp^2 hybridization for the iron center of $(Cl_8TPP)Fe^{III}$–OH. As such, two of the sp^2 electrons form two metal–pyrrole nitrogen covalent bonds and the remaining electron forms a metal–hydroxyl covalent bond (PFe–OH; bonding that is similar to that for H–OH and R–OH).

In the presence of excess $^-$OH an adduct is formed, $[(H\text{-}O^-)(Cl_8TPP)Fe^{III}\text{–}OH]^-$, with the ligand field of $^-$OH inducing an in-plane octahedral geometry and an intermediate spin state ($S = {}^3/_2$) (Tables I and II). The electrochemical data (Figures 1–3 and Table II) and the magnetic data are consistent with the conclusion that oxidation of $^-$OH in the presence of $(Cl_8TPP)Fe^{II}(^-OH)^-$, $(Cl_8TPP)Mn^{II}$, and $(Cl_8TPP)^{II}Co^{\bullet}$ yields $^{\bullet}$OH, which couples with an unpaired d electron and thereby reduces the magnetic moment of the metalloporphyrin by about 1 μ_B (and the spin state by ${}^1/_2$; see Table II). Thus, the redox and magnetic data support the conclusion that electron-transfer oxidation for the $^-$OH adducts for these metalloporphyrins is ligand-centered and facilitated by d–p covalent bond formation between the metal center and $^{\bullet}$OH.

$O_2^{\bullet-}$ Adducts. PZn. The oxidation of $O_2^{\bullet-}$ in the presence of $(Cl_8TPP)Zn$ occurs at a slightly more positive potential than that for free $O_2^{\bullet-}$. Because $(Cl_8TPP)Zn$ (with $d^{10}sp$ valence-electron hybridization) does not offer any means to stabilize an $O_2^{\bullet-}$ adduct, $^-$OH is favored because of its greater basicity (larger charge density on oxygen; the negative charge of $O_2^{\bullet-}$ is delocalized over both oxygens). Hence, there is no change in the UV–visible spectrum of $(Cl_8TPP)Zn(^-OH)^-$ when $O_2^{\bullet-}$ is introduced.

PFe. The sensitivity of $PFe(O_2)^-$ to degradation by trace levels of water ($2O_2^{\bullet-} + HOH \rightarrow HOO^- + O_2 + {}^-OH$) has been demonstrated.[8,11,48] In the present study the acidity of the medium[30,31] has been attenuated by the presence of excess $^-$OH, which enhances the stability of $(Cl_8TPP)Fe(O_2)^-$. The absence of reactions by this $O_2^{\bullet-}$ adduct with the solvent medium is confirmed by the essentially identical electrochemical and spectroscopic results obtained in DMF and MeCN; the latter has been successfully employed in the magnetic and spectroscopic characterization of $(OEP)Fe(O_2)^-$.[11] The UV–visible spectrum of $(Cl_8TPP)Fe(O_2)^-$ is essentially the same as that for $(TPP)Fe(O_2)^-$ (TPP = tetraphenylporphyrin),[4,11] and its magnetic moment is similar to that for other $PFe(O_2)^-$ adducts.[8,11] The Soret band of $(Cl_8TPP)Fe^{II}$ is slightly red-shifted upon $^-$OH coordination, as expected for a singly charged ligand anion. Formation of $(Cl_8TPP)Fe(O_2)^-$ results in a comparable red-shift, which is consistent with a monoanionic formulation ($O_2^{\bullet-}$) rather than a dianion (O_2^{2-}).[11]

Oxidation of $(Cl_8TPP)Fe(O_2)^-$ ($E^{\circ\prime} = -0.36$ V) occurs at a more positive potential than that for free $O_2^{\bullet-}$ ($E^{\circ\prime} = -0.88$ V) [or for $O_2^{\bullet-}$ in the presence of $(Cl_8TPP)Zn$]. This stabilization to electron removal is the result of covalent bond formation between an unpaired p electron of $O_2^{\bullet-}$ and an unpaired d electron of $(Cl_8TPP)Fe^{II}$ to give $(Cl_8TPP)Fe^{III}$–OO^-, which is analogous to the stabilization of $^{\bullet}$OH via coupling with $(Cl_8TPP)Fe^{II}$ to give $(Cl_8TPP)Fe^{III}$–OH (both have iron centers with d^5sp^2 valence-electron hybridization and $S = {}^5/_2$ spin states). The extent of stabilization, estimated by the shift in the $O_2^{\bullet-}$ oxidation potential (see Table II), is 12 kcal ($-\Delta G_{BF}$). The generation of O_2 upon oxidation of $(Cl_8TPP)Fe^{III}$–OO^- is supported by its characteristic reduction at –0.88 V (Figure 1d). The irreversible reduction at –1.21 V is consistent with the dissociation of the oxygen species from $(Cl_8TPP)Fe^{II}$ to give $^-$OOH, which reacts with Me_2SO to give Me_2SO_2 and $^-$OH[49] and with CH_3CN to give $CH_3C(O\text{-}H)(O^-)NH_2$.[31,50,51] Because (a) $^-$OH is more difficult to oxidize than $O_2^{\bullet-}$ (Table II) and (b) oxidation of the $^-$OH adducts of metalloporphyrins is ligand-centered, the oxidation of $(Cl_8TPP)Fe^{III}$–OO^- must be ligand-centered (the liberation of O_2 upon a one-electron oxidation is consistent with this conclusion). The electron affinities for $O_2^{\bullet-}$ and $((Cl_8TPP)Fe^{II})^+$, which are directly proportional to their one-electron electron-transfer reduction potentials [$((Cl_8TPP)^{II})^+$ ($E^{\circ\prime}_{DMF} = -0.06$ V vs SCE) > O_2 (–0.88 V) > $(Cl_8TPP)Fe^{II}$ (–0.98 V) > $O_2^{\bullet-}$ (<–1.64 V)], preclude the formation of $[((Cl_8TPP)Fe^{II})^+(O_2^{2-})]^-$. Hence, there is no significant electron transfer between $O_2^{\bullet-}$ and $(Cl_8TPP)Fe^{II}$ when they are combined.

The interpretations[4] of the vibrational data for $PFe(O_2)^-$ need to be reconsidered in relation to the preceding arguments for covalent bonding between PFe^{II} and $O_2^{\bullet-}$. Free $O_2^{\bullet-}$ (gas phase) has an O–O vibrational energy of 1065 cm^{-1} and a bond order of 1.5; addition of an H$^{\bullet}$ atom to $O_2^{\bullet-}$ gives a covalent HOO^- molecule and reduces the O–O bond order to 1.0 with an HO–O^- vibrational energy of 836 cm^{-1} [H–OO^- bond energy (ΔH_{DBE}) 80 kcal];[52] the HO–OH vibrational energy is 877 cm^{-1} (H–OOH bond energy 88 kcal).[53] The pattern indicates that formation of covalent bonds causes the O–O stretching vibrational frequency to decrease relative to that for $O_2^{\bullet-}$ and that there is an apparent direct relationship between the H–O covalent bond energy and the O–O stretching frequency. Thus, the estimated covalent bond energy ($\Delta H_{DBE} = 20$ kcal; Table II)[54] for the $(Cl_8TPP)Fe^{III}$–OO^- bond is consistent with the 836-cm^{-1} O–O vibrational frequency for $(OEP)Fe(O_2)^-$.[4] The lower PFe^{III}–OO^- bond energy (relative to that for the H–OO^- bond) is in accord with the expectation that the d^6sp valence-electron hybridization of PFe^{II} provides a lower electron spin density than H$^{\bullet}$ (1s).

The magnetic moment for $(Cl_8TPP)Fe(O_2)^-$ (5.57 μ_B, $S = {}^5/_2$) and the absence of any outer-sphere propensity for electron-transfer between $(Cl_8TPP)Fe^{II}$ and $O_2^{\bullet-}$ (Table II), as well as other magnetic and spectroscopic evidence,[8,11] are consistent with d^5sp^2 hybridization for the iron center of $(Cl_8TPP)Fe(O_2)^-$. As such, the bonding is analogous to that for $(Cl_8TPP)Fe^{III}$–OH with a metal–superoxide covalent bond (PFe^{III}–OO^-; bonding that is similar to that for H–OO^- and Bu–OO^-).

The –0.18-V difference in the formal reduction potentials for the $(Cl_8TPP)Fe^{III}$–OH/$(Cl_8TPP)Fe^{II}(^-OH)^-$ couple ($E^{\circ\prime} = -0.70$ V) and the $O_2/O_2^{\bullet-}$ couple ($E^{\circ\prime} = -0.88$ V) indicates that stabilization of $O_2^{\bullet-}$ via covalent-bond formation with $(Cl_8TPP)Fe^{III}$–OH (4 kcal or more) will favor reduction of O_2 by $(Cl_8TPP)Fe^{II}(OH)^-$. Because the apparent $(Cl_8TPP)Fe^{III}$–OO^- bond energy is 12 kcal ($-\Delta G_{BF}$, Table II), the combination of $(Cl_8TPP)Fe^{II}$ (d^6sp, $S = {}^4/_2$), O_2, and $^-$OH should result in the exothermic formation of $(Cl_8TPP)Fe^{IV}(OH)(OO^-)$ with Fe–OH and Fe–OO^- covalent bonds. The observed magnetic moment (2.91 μ_B, $S = {}^2/_2$; Table I) for the product solution from this combination, as well as the electrochemistry and UV–visible spectroscopy, are consistent with this formulation. Electrochemical oxidation at 0.0 V of the product solution yields O_2 and $(Cl_8TPP)Fe^{III}$–OH, which provides further support for the spontaneous formation of this species.

$$(Cl_8TPP)Fe^{II} + O_2 + {}^-OH \longrightarrow (Cl_8TPP)Fe^{IV}\begin{matrix}\text{OH}\\ \text{OO}^-\end{matrix} \quad (7)$$

This reaction represents a unique and perhaps the first example of actual electron transfer between an iron porphyrin and dioxygen and offers a means for oxygen transport and storage.

Because $(Cl_8TPP)Fe^{III}$–OO^- and $(Cl_8TPP)Fe^{IV}(OH)(OO^-)$ are strong nucleophilic bases, excess $^-$OH is required to stabilize them from reaction with trace levels of water in the solvent. In the

(47) Richert, S. A.; Tsang, P. K. S.; Sawyer, D. T. *Inorg. Chem.* **1989**, *28*, 2471.
(48) VanAtta, R. B.; Strouse, C. E.; Hanson, L. K.; Valentine, J. S. *J. Am. Chem. Soc.* **1987**, *109*, 1425.
(49) Goolsby, A. D.; Sawyer, D. T. *Anal. Chem.* **1968**, *40*, 83.
(50) Roberts, J. L., Jr.; Morrison, M. M.; Sawyer, D. T. *J. Am. Chem. Soc.* **1978**, *100*, 329.
(51) Sawaki, Y.; Ogata, Y. *Bull. Chem. Soc. Jpn.* **1981**, *54*, 793.
(52) The H–OO^- bond energy (ΔH_{DBE}) has a value of 80.1 kcal on the basis of electrochemical data (H_2O, pH 14); $O_2^{\bullet-} + HOH + e^- \rightarrow H\text{–}OO^- + {}^-OH$ ($E^{\circ} = +0.20$ V vs NHE), $HOH + e^- \rightarrow H^{\bullet} + {}^-OH$ ($E^{\circ} = -2.93$ V vs NHE), and $\Delta H_{DBE} = -\Delta G_{BF} + T\Delta S_{DBE} = \Delta E^{\circ}$ (23.1 kcal/eV) + 7.8 kcal = 80.1 kcal. Sawyer, D. T. *J. Phys. Chem.* **1989**, *93*, 7977.
(53) Shum, L. G. S.; Benson, S. W. *J. Phys. Chem.* **1983**, *87*, 3479.
(54) $\Delta H_{DBE} = -\Delta G_{BF} + T\Delta S = 12 + 8 = 20$.

absence of ^-OH reductive electrolysis of $[(Cl_8TPP)Fe^{II} + O_2]$ yields $(Cl_8TPP)Fe^{III}$–OH as the major product. A plausible water-induced decomposition pathway is outlined by eq 8 (analogous to that for $O_2^{\bullet-}$).[55] The decomposition path for $(Cl_8TPP)Fe^{IV}(OH)(OO^-)$ in the absence of excess ^-OH probably is similar to that for $(Cl_8TPP)Fe^{III}$–OO^- (eq 8).

$$(Cl_8TPP)Fe^{II} + O_2 + e^- \longrightarrow (Cl_8TPP)Fe^{III}\text{–}OO^- \xrightarrow{H_2O} (Cl_8TPP)Fe^{III}\text{–}OOH + {}^-OH \quad (8)$$

$$(Cl_8TPP)Fe^{III}\text{–}OOH \xrightarrow{H_2O} (Cl_8TPP)Fe^{III}\text{–}OH + HOOH$$

The much-proposed PFe(O) intermediate in the cytochrome P-450 reaction cycle (Scheme I) has an Fe–O bond energy of 74 kcal,[56] which precludes O-atom transfer to organic substrates. The instability of $(Cl_8TPP)Fe^{III}$–OOH (Fe–OOH bond energy less than 20 kcal mol^{-1}) makes it a viable reactive intermediate for the cytochromes P-450; $HO_2^{\bullet}$ is a potent oxidant, and a stabilized $HO_2^{\bullet}$ generated from the cytochrome P-450 catalytic cycle affords a more efficient system for oxygenation of substrates. A plausible reaction cycle includes its transient formation in the presence of bound substrate (R'H).

$$(RS)PFe^{III} \xrightarrow{R'H} (RS)PFe^{III}(R'H) \xrightarrow{H^+, e^-} \xrightarrow{O_2} [(RS)PFe^{IV}\text{–}OOH](R'H)] \xrightarrow{H^+, e^-} (RS)PFe^{III} + R'OH + H_2O \quad (9)$$

PMn and PCo. Electrochemical oxidation of $(Cl_8TPP)Mn(O_2)^-$ ($E^{\circ\prime}$ = −0.13 V) liberates O_2, and the shift to a more positive potential relative to that for free $O_2^{\bullet-}$ is analogous to the behavior of $(Cl_8TPP)Fe^{III}$–OO^-. Thus, covalent-bond formation between an unpaired p electron of $O_2^{\bullet-}$ and an unpaired d electron of PMn^{II} (d^5sp) provides stabilization of about 17 kcal (Table III).

The observed magnetic moment for $(Cl_8TPP)Mn^{III}$–OO^- (4.98 μ_B; Table I) is the same as that for $(TPP)Mn(O_2)^-$,[8] which has been formulated as $(TPP)Mn(O_2^{\bullet-})^-$.[8,57] A recent X-ray crystallographic structure determination[48] for $(TPP)Mn(O_2)^-$ has an O–O bond distance that is interpreted to be indicative of a O_2^{2-} dianion. However, the preceding arguments for a reinterpretation of the vibrational data for $PFe(O_2)^-$ also apply to O–O bond distances. Thus, the O–O bond distances should be similar for H–OO–H, Na^+OO^-Na, H–OO^-, and $(TPP)Mn^{III}$–OO^- (all with a bond order of 1).

The generation of stable solutions of $(Cl_8TPP)Mn^{III}$–OO^- by reduction of $[(Cl_8TPP)Mn^{II} + O_2]$ does not require the presence of ^-OH during the electrolysis, which is consistent with the greater stability of $PMn(O_2)^-$ to moisture relative to $PFe(O_2)^-$[8,11,48] and its larger $(Cl_8TPP)Mn^{III}$–OO^- bond energy. An analogous species is not generated when $(Cl_8TPP)Mn^{II}$, ^-OH, and O_2 are combined despite the favorable stabilization (17 kcal) that results from $(Cl_8TPP)Mn^{III}$–OO^- formation. This probably is due to the less negative reduction potential for the $(Cl_8TPP)Mn^{III}$–OH/$(Cl_8TPP)Mn^{II}(^-OH)^-$ couple [−0.43 V versus −0.70 V for $(Cl_8TPP)Fe^{III}$–OH].

Because the formal reduction potential for the $(Cl_8TPP)Co^{II}/((Cl_8TPP)Co^{II})^-$ couple is more positive than that for the $O_2/O_2^{\bullet-}$ couple, direct electrolytic reduction of $(PCo^{II} + O_2)$ cannot be applied. However, the $(Cl_8TPP)Co(O_2)^-$ species is generated at the electrode surface when a negative voltage scan is applied to a solution that contains $((Cl_8TPP)Co^{II})^{\bullet}$, ^-OH, and O_2. The reduction products, $O_2^{\bullet-}$ and $((Cl_8TPP)Co^{II})^-$ (E_{red} < −1.4 V), yield $(Cl_8TPP)Co(O_2)^-$ upon reoxidation. The weak $(Cl_8TPP)Co^{II}$–OO^- bond (7 kcal) necessitates the presence of ^-OH to preclude decomposition via hydrolysis (eq 8). The formal reduction potential for the $(Cl_8TPP)Co^{III}$–OH/$(Cl_8TPP)Co^{II}(^-OH)^-$ couple, the small PCo^{III}–OO^- bond energy, and its valence-electron hybridization (d^6sp^2) preclude $(Cl_8TPP)Co(OH)(OO^-)$ formation.

O_2 Adduct. The electrochemistry (Figure 4) and spectroscopy for the combination of O_2 and metalloporphyrins indicate the absence of interaction between O_2 and $(Cl_8TPP)Zn^{II}$, $(Cl_8TPP)Mn^{II}$, and $((Cl_8TPP)Co^{II})^{\bullet}$. However, the positive shift of the potential for O_2 reduction (Figure 4c) is due to binding of O_2 to $(Cl_8TPP)Fe^{II}$, as is the small shift in the potential for $(Cl_8TPP)Fe^{II}$ oxidation in the presence of O_2. These results confirm that formation of $(Cl_8TPP)Fe(O_2)$ is not accompanied by electron transfer from $(Cl_8TPP)Fe^{II}$ to O_2. Furthermore, the reduction potential for the $O_2/O_2^{\bullet-}$ couple is more negative than that for the $((Cl_8TPP)Fe^{III})^+/(Cl_8TPP)Fe^{II}$ couple ($O_2^{\bullet-}$ is used to reduce PFe^+ to PFe). The O–O bond lengths and O–O vibrational frequencies for $PFe(O_2)$ and oxyhemoglobin can be rationalized by arguments that are similar to those presented for the bonding of $(Cl_8TPP)Fe^{III}$–OO^-. Thus, the two unpaired electrons of $^3O_2$ couple with two of the four unpaired d electrons of $(Cl_8TPP)Fe^{II}$ (d^6sp, $S = {}^4/_2$) to form two weak covalent bonds and give

d^6sp, $S = 0$; L = DMF

The irreversible reduction of O_2 in the presence of $(Cl_8TPP)Mn^{II}$ and the current enhancement for the oxidation of $(Cl_8TPP)Mn^{II}$ on the reverse scan are consistent with $(Cl_8TPP)Mn^{III}$–OO^- formation from $(PMn + O_2^{\bullet-})$. The small current increase for the $((Cl_8TPP)Co^{II})^{\bullet}/((Cl_8TPP)Co^{II})^-$ couple in the presence of O_2 appears to be due to the reoxidation of $(Cl_8TPP)Co^-$ by O_2.

The electrochemical, spectroscopic, and magnetic results for the $^{\bullet}OH$, $O_2^{\bullet-}$, and O_2 adducts of $(Cl_8TPP)M$ (M = Fe, Mn, Co) are consistent with the conclusion that the site of electron transfer is oxygen-centered and that the oxygen species are stabilized by covalent-bond formation between an unpaired d electron of the transition metal and an unpaired p electron of oxygen. The electrochemistry and magnetic moment for $(Cl_8TPP)Fe^{III}$–OO^- indicate that the valence electrons of the iron center are hydridized to d^5sp^2. The formation of a covalent bond between an iron atom and an oxygen species ($O_2^{\bullet-}$) is analogous to such bond formation between a hydrogen atom and an oxygen species to give H–OO^- ($H^{\bullet} + O_2^{\bullet-}$). The concept of valence-electron hybridization to achieve more effective bonding with iron is equivalent to that for the carbon atom ($s^2p^2 \rightarrow sp^3$).

The activation of the O–O bond by cytochromes P-450 is proposed to involve a stabilized $HOO^{\bullet}$ species rather than an iron-stabilized oxygen atom [PFe(O)]. The difficulties in the isolation and study of the reactive intermediate of cytochromes P-450 are consistent with an unstable, highly reactive PFe–OOH species. Work is in progress to characterize the reactivity of $(Cl_8TPP)Fe^{III}$–OO^- and $(Cl_8TPP)Fe^{III}$–OOH in relation to the reaction cycle of cytochrome P-450.

The present study also provides insight into the mechanisms for superoxide ion disproportionation that are catalyzed by the iron and manganese superoxide dismutase proteins. The combination of PFe^{II} or PMn^{II} with $O_2^{\bullet-}$ does not result in electron transfer from the metal; instead they couple to form PFe^{III}–OO^- and PMn^{III}–OO^-. The latter abstract protons from the medium, and the PFe^{III}–OOH and PMn^{III}–OOH products react with a second $O_2^{\bullet-}$ and a proton to give HOOH and O_2 (eq 10). Thus,

$$PFe^{II} + O_2^{\bullet-} + HA \longrightarrow PFe^{III}\text{–}OOH + A^- \xrightarrow{O_2^{\bullet-}, HA} PFe^{II} + O_2 + HOOH + A^- \quad (10)$$

PFe^{II} and PMn^{II} facilitate the disproportionation of $O_2^{\bullet-}$, which is equivalent to the function of the iron and manganese superoxide

(55) $2O_2^{\bullet-} + H_2O \rightarrow O_2 + HOO^- + {}^-OH$. Ref 39 and: Sugimoto, H.; Sawyer, D. T. Unpublished results.
(56) Sugimoto, H.; Tung, H.-C.; Sawyer, D. T. *J. Am. Chem. Soc.* **1988**, *110*, 2465.
(57) Valentine, J. S.; Quinn, A. E. *Inorg. Chem.* **1976**, *15*, 1997.

dismutase proteins. Whether the mechanism suggested by eq 10 is relevant to those for the proteins is unknown, but the absence of electron transfer from their metal centers to $O_2^{\bullet-}$ is a reasonable expectation.

Acknowledgment. This work was supported by the National Science Foundation under Grant No. CHE-8516247. We are grateful to the Robert A. Welch Foundation for the award of a Predoctoral Fellowship to P.K.S.T.

Contribution from the Institute for Inorganic Chemistry, University of Witten/Herdecke, Stockumer Strasse 10, 5810 Witten, Federal Republic of Germany

Influence of the Pendant Group on the Substitution Lability of N-Substituted Ethylenediaminetriacetate Complexes of Ruthenium(III) in Aqueous Solution

H. C. Bajaj[1] and R. van Eldik*

Received July 13, 1989

Following earlier studies on the substitution behavior of ethylenediaminetetraacetate and related complexes of Ru(III), the series has now been extended to include data for the *N*-methylethylenediaminetriacetate complex. Substitution reactions of the aqua and hydroxo complexes with thiocyanate and thiourea exhibit remarkably different activation volumes, which suggest that the substitution mechanism may change over from I_a to A for the aqua and hydroxo complexes, respectively. These data enable an overall discussion of the influence of the pendant group on the substitution lability of such ruthenium(III) complexes. It is suggested that when the pendant group contains a carboxylate moiety, the syn lone pair of electrons on the carboxylate oxygen may interact effectively with the coordinated water molecule and so account for the extreme lability observed in the case of the ethylenediaminetetraacetate complex.

Introduction

The extreme lability of the Ru(edta)H_2O^- complex (edta = ethylenediaminetetraacetate) has attracted significant attention from kineticists in recent years.[2-6] In these studies it is generally accepted that edta is coordinated as a pentadentate ligand with the sixth coordination site being occupied by a water molecule. Protonation of the pendant carboxylate group (i.e. R = CH_2COO^- in **1**) or deprotonation of the coordinated water molecule results

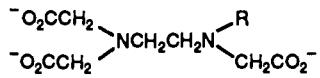

1

in a substantial decrease in the lability of the Ru(edta)H_2O^- complex.[3-6] It is especially the role of the pendant R group that has stimulated interesting research in this area.[6-8]

We recently reported a detailed study of the substitution behavior of Ru(edta)H_2O^- with a series of anionic and neutral ligands.[6] The reported activation parameters, especially ΔV^*, support the operation of an I_a mechanism in which the pendant carboxylate moiety significantly assists Ru–OH_2 bond breakage. We concluded that hydrogen bonding between the carboxylate oxygen and the coordinated water molecule could account for the increased lability. This could result in a weakening of the Ru–OH_2 bond and/or in the creation of an open area and accessible site for associative ligand attack. In order to gain more insight into the influence of the pendant R group in **1**, we performed a kinetic study of the substitution behavior of Ru(hedtra)H_2O, where hedtra = *N*-(hydroxyethyl)ethylenediaminetriacetate (i.e. R = CH_2CH_2OH in **1**).[7] In this way, the suggested effect of hydrogen bonding could be reduced and the protonation of the pendant R group could be excluded. The results demonstrated a decrease of approximately 2 orders of magnitude in the substitution rate constant of the aqua complex as compared to the edta analogue. The activation parameters underline the operation of an I_a mechanism.

In the present study, we have replaced R in **1** by methyl in order to even further decrease the possible effect of hydrogen bonding between R and the coordinated water molecule. The results of this investigation, along with those reported before,[6,7] enable us to comment on the intimate nature of the pendant labilization effect and to reveal mechanistic differences between the substitution behavior of Ru(medtra)H_2O and Ru(medtra)OH^-, where medtra = *N*-methylethylenediaminetriacetate.

Experimental Section

Materials. An aqueous concentrated solution of Na_3medtra was prepared as described elsewhere[9] by the reaction of *N*-methylethylenediamine with monochloroacetic acid. Since the ligand could not be readily isolated, this solution was used in the subsequent synthetic work. A portion of this solution (2.0 mmol) acidified to pH 4 with concentrated HCl was added to 0.75 g (2.0 mmol) of $K_2[RuCl_5H_2O]$, and the mixture was refluxed for 2 h. During this time, the solution became greenish yellow. It was reduced in volume on a water bath, followed by the addition of cold ethanol to precipitate the complex. The precipitate was filtered off, washed with cold ethanol/water (9:1), and dried under vacuum. The yield based on $K_2[RuCl_5H_2O]$ was 45%. Chemical analysis[10] for K[Ru(medtra)Cl]·$2H_2O$ (theoretical values): C, 24.18 (23.66); H, 3.86 (3.72); N, 5.66 (6.13). All other chemicals were of analytical reagent grade, and deionized water (Millipore) was used throughout this study. Acetate, citrate, phosphate, and borate buffers were used to control the pH of the test solutions.[11] Na_2SO_4 was used to adjust the ionic strength.

Measurements. The substitution reactions were followed spectrophotometrically in the wavelength range 360–600 nm with a Shimadzu UV 250 spectrophotometer and a Durrum D 110 stopped-flow instrument. Kinetic measurements at elevated pressure were performed on a

(1) On leave from the Central Salt and Marine Chemicals Research Institute, Gijubhai Badheka Marg., Bhavnagar 364002, India.
(2) Matsubara, T.; Creutz, C. *J. Am. Chem. Soc.* **1978**, *100*, 6255.
(3) Matsubara, T.; Creutz, C. *Inorg. Chem.* **1979**, *18*, 1956.
(4) Yoshino, Y.; Uehiro, T.; Saito, M. *Bull. Chem. Soc. Jpn.* **1979**, *52*, 1060.
(5) Toma, H. E.; Santos, P. S.; Mattioli, M. P. D.; Oliveira, L. A. A. *Polyhedron* **1987**, *6*, 603.
(6) Bajaj, H. C.; van Eldik, R. *Inorg. Chem.* **1988**, *27*, 4052.
(7) Bajaj, H. C.; van Eldik, R. *Inorg. Chem.* **1989**, *28*, 1980.
(8) Ogino, H.; Masuko, A.; Ito, S.; Miura, N.; Shimura, M. *Inorg. Chem.* **1986**, *25*, 708.
(9) Van Saun, C. W.; Douglas, B. E. *Inorg. Chem.* **1968**, *7*, 1393.
(10) Beller Microanalytical Laboratory, Göttingen, FRG.
(11) Perrin, D. D.; Dempsey, B. *Buffers for pH and metal ion control*; Chapman and Hall: London, 1974.

0020-1669/90/1329-2855$02.50/0